



*Citation for published version:*

Singh, M, Kurchania, R, Ball, RJ & Sharma, GD 2016, 'Efficiency enhancement in dye sensitized solar cells through step wise cosensitization of TiO<sub>2</sub> electrode with N719 and metal free dye', Indian Journal of Pure & Applied Physics, vol. 54, pp. 656-664.

*Publication date:*  
2016

*Document Version*  
Publisher's PDF, also known as Version of record

[Link to publication](#)

*Publisher Rights*  
CC BY-NC-ND

## University of Bath

### General rights

Copyright and moral rights for the publications made accessible in the public portal are retained by the authors and/or other copyright owners and it is a condition of accessing publications that users recognise and abide by the legal requirements associated with these rights.

### Take down policy

If you believe that this document breaches copyright please contact us providing details, and we will remove access to the work immediately and investigate your claim.

## Efficiency enhancement in dye sensitized solar cells through step wise cosensitization of TiO<sub>2</sub> electrode with N719 and metal free dye

Manjeet Singh<sup>a</sup>, Rajnish Kurchania<sup>a</sup>, R J Ball<sup>b</sup> & G D Sharma<sup>c\*</sup>

<sup>a</sup> Department of Physics, Maulana Azad National Institute of Technology (MANIT),  
Bhopal 462 051, India

<sup>b</sup> Department of Architecture and Civil Engineering, University of Bath, Bath BA2 7AY,  
United Kingdom

<sup>c</sup> Department of Physics, LNM Institute of Information Technology (Deemed University)  
Jamdoli, Jaipur 303 101, India

Received 26 September 2014; revised 30 August 2016; accepted 12 December 2016

We have used a step-wise cosensitization process to improve the power conversion efficiency (PCE) of dye sensitized solar cells employing N719 and metal free dye TA-St-CA. The DSSC sensitized with N719/TA-St-CA shows a PCE of 8.27% which is higher than for the DSSCs sensitized with either N719 (5.78 %) or TA-St-CA (4.45%). The improved PCE is attributed to the enhanced overall dye loading as well the reduced dye aggregation that has resulted from the usage of dyes with different anchoring units. The enhancement in the PCE has also been attributed to increase in both short circuit photocurrent and open circuit voltage. This was due to the reduced dark current and suppression of back recombination of injected electrons in the conduction band of TiO<sub>2</sub> photoanode with the I<sub>3</sub><sup>-</sup> ions in the electrolyte.

**Keywords:** Cosensitization, Dye sensitized solar cells (DSSC), Dye loading, Power conversion efficiency

### 1 Introduction

Dye sensitized solar cells (DSSCs) are currently attracting worldwide scientific interest due to their low cost, high efficiency and simple fabrication methods and environmental friendly nature which have been regarded as a promising alternative to conventional silicon solar cells, since they were reported by O'Regan and Gratzel<sup>1-3</sup> in 1991. Record power conversion efficiency (PCE) of 12.3 % has been achieved for DSSC's based on a donor- $\pi$ -acceptor type zinc porphyrin and cobalt-based type electrolyte<sup>4</sup>. However, this PCE is still lower than that of silicon based solar cells, and further improvement is necessary for their commercial applications<sup>5</sup>. A typical DSSC consists of four main components, namely, the sensitizer, nano-crystalline metal oxide semiconductor (usually TiO<sub>2</sub> and ZnO) electrode, redox mediator and counter electrode. Although optimization of each components mentioned above plays an important role for achieving the higher PCE<sup>6</sup>, much research is focusing on the synthesis and development of new sensitizers, since they are crucial

for the improvement of PCE of the DSSC<sup>3,7-9</sup>. In general, three types of dyes, i.e., ruthenium polypyridyl dyes<sup>10-12</sup>, porphyrin dyes<sup>13-15</sup> and organic metal free dyes<sup>16-18</sup> were used as sensitizers for most of the DSSCs. In the DSSC, a sensitizing dye adsorbed onto the surface of a nano-crystalline TiO<sub>2</sub>, absorbs the light to inject an electron to the conduction band of TiO<sub>2</sub>, followed by the dye regeneration by the redox couple in electrolyte or a solid state hole conductor. In order to improve the PCE of DSSCs, the sensitizer should be panchromatic, that is absorb photons from the solar spectrum ranging from visible to near infrared, while maintaining sufficient driving force for electron injection and dye regeneration processes. Recent research has concentrated on improving the spectral response of the individual dyes by synthesizing panchromatic dyes such as black dye<sup>19-22</sup>, increasing  $J_{sc}$  has been achieved at the expense of  $V_{oc}$ , and limited this approach. Moreover, single dyes with a wide absorption spectrum commonly have difficulty injecting the photogenerated electrons from the sensitizer to the photoanode. This is commonly observed when the TiO<sub>2</sub> conduction band is approaching the dyes LUMO level<sup>23,24</sup>.

\*Corresponding author (E-mail: sharmagd\_in@yahoo.com, gdsharma273@gmail.com)

Cosensitization is an effective approach to achieve the panchromatic collection behavior of the photoelectrodes<sup>25-32</sup>. The performance of the DSSC can be enhanced through a combination of the two or more dyes attached to the nano-crystalline semiconductor film, extending the light harvesting efficiency so to increase the photocurrent in the DSSCs. However, the selection of co-sensitizers used in DSSCs is a challenging task with respect to preventing competitive adsorption and unfavorable aggregation of dyes that may reduce the photocurrent or voltage of DSSCs.

The Ru dye based DSSCs showed relatively lower incident photon to current efficiency values in the 400-480 nm wavelength regions compared to the 500-650 nm wavelength regions. This is due to the competitive light absorption by the tri-iodide used in the electrolyte, since tri-iodide showed an absorption band around 420 nm. This strongly affects the light harvesting efficiency of Ru based dyes such as N719 due to its relatively low molar extinction coefficient relative to tri-iodide<sup>33,34</sup>. Therefore, the ideal co-sensitizer to be used should efficiently harvest light in this region, i.e., 400-480 nm and should have a smaller molecular size to permit the coadsorption with N719 dye onto the TiO<sub>2</sub> surface. Moreover, it should effectively suppress the electron recombination with I<sub>3</sub><sup>-</sup> and dye aggregation. Han *et al.*<sup>30</sup> have used a metal free dye having a structure donor- $\pi$ -acceptor (D- $\pi$ -A) as a co-sensitizer with black dye and achieved a certified PCE of 11.4 % and recently about 11.6 %. The simplest method for cosensitization is to sensitize the photoelectrode with solution containing multiple dyes, i.e., a dye cocktail. However, different speeds of dye uptake, molecular sizes of dyes and affinities of the dyes to the TiO<sub>2</sub> surface increase the unfavorable interactions such as electron transfer and electron-hole recombination between the adsorbed dyes near to the photoanode<sup>35-37</sup>.

An inexpensive and simple method of cosensitization of a single TiO<sub>2</sub> electrode using a number of sensitizers is the step wise adsorption of selective dyes<sup>39-40</sup>. This paper details a DSSC system exploiting the well-known N719, Ru based dye, and the metal free dye TA-St-CA. Through the use of these dyes as primary and secondary sensitizers, respectively, cosensitization was achieved using a step wise adsorption approach. This led to the PCE of the DSSCs increasing. A PCE of approximately 8.27 % was achieved for the N719/TA-St-CA cosensitized DSSC which was higher compared to those based

either TA-St-CA (4.45%) or N719 (5.78 %) sensitizer. Both the open circuit voltage  $V_{oc}$  and short circuit photocurrent  $J_{sc}$  were enhanced leading to the observed improvement in PCE.

## 2 Experimental Details

Decon 90, distilled water, isopropanol and ethanol were used in conjunction with sonication to clean substrates of fluorine doped tin oxide (FTO) glass. The DSSC working electrodes were manufactured by initially creating a blocking layer by applying 0.2M di-isopropoxy titanium *bis* (acetylacetonate) dissolved in isopropanol using spray pyrolysis. Subsequently the doctor blade technique was used to deposit a TiO<sub>2</sub> nano-crystalline layer of Dyesol TiO<sub>2</sub> paste (DSL 18NR-T) on the clean substrate of FTO coated glass. This coating was then stabilized by heated to 500 °C for 30 min.

A 0.02 M aqueous solution of TiCl<sub>4</sub> was prepared and the TiO<sub>2</sub> electrodes were then dipped for 20 min before rinsing with water and ethanol. The electrodes were then annealed at a temperature of 500 °C for 20 min. A thin film thickness measurement system (Nano calc XR Ocean Optics Germany) was used to determine the electrode thickness, which was found to be in the range 10-12  $\mu$ m.

Dye solutions were produced by mixing a  $5 \times 10^{-4}$  M dye TA-St-CA in THF and  $3 \times 10^{-4}$  M N719 in acetonitrile/tert-butanol (1:1 v/v). Cosensitization was achieved by dipping the TiO<sub>2</sub> photoanode firstly into the N719 solution for a duration of 4 h and then subsequently rinsing with ethanol before then dipping into the solution of TA-St-CA for a further 4 h. Spin coating was used to prepare the counter electrode from a H<sub>2</sub>PtCl<sub>4</sub> solution (2mg of Pt in 1ml of isopropanol) onto a substrate of pre-cleaned FTO coated glass. Following coating the glass was heated to 450 °C for 15 min in air. The test cell was produced using a sandwich type configuration formed from the counter electrode and a Pt coated FTO working electrode. Sealing of the cell was achieved using Surllyn hot melt polymer adhesive. DSSC fabrication was completed by introducing an electrolyte solution containing I<sub>2</sub> (0.03 M), LiI (0.05M), 0.5 M tert-butylpyridine and 1 methyl-3-n-propylimidazolium iodide (0.6 M ) in a mixture of acetonitrile and valeronitrile (85:15 volume ratio) into the cavity between the two electrodes. To ensure complete penetration of the liquid, vacuum backfilling was used through a hole drilled in the Pt coated FTO. Duplicate cells as described above were prepared for comparison to

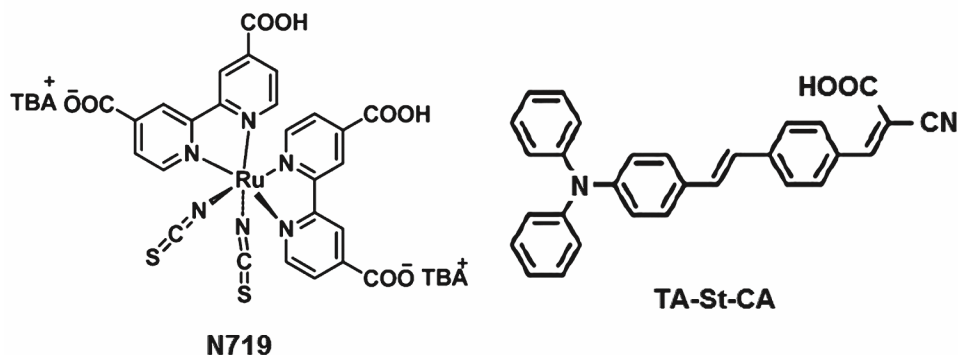
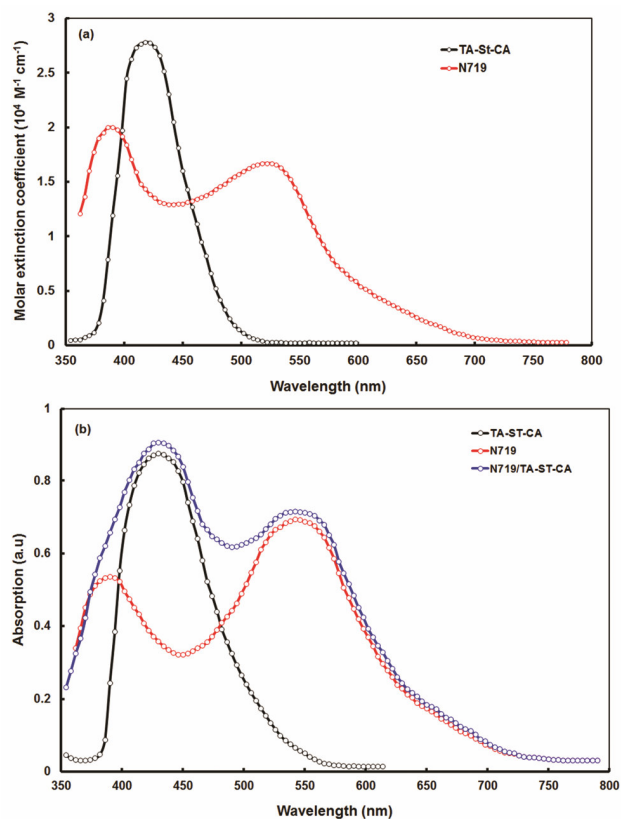


Fig. 1 – Chemical structure of N719 and TA-St-CA dyes

increase the statistical significance of the results. In addition the influence of the order of dye application on performance was investigated by manufacturing cells cosensitized by firstly dipping into the TA-St-CA, followed by the N719 solution. A computer controlled Keithley source meter (2601 A) was used to determine the current –voltage ( $J$ - $V$ ) characteristics when the cells were illuminated using a solar simulator TS space system class AAA under an illumination of AM1.5, 100 mW/cm<sup>2</sup>. A Bentham IPCE system (TMc 300 monochromator computer controlled) was then employed to measure the incident photon to current efficiency (IPCE) spectra. An Autolab potentiostat/Galvanostat PGSTAT30 recorded cyclic voltammogram curves to characterize the electrochemical performance of the DSSCs. A scan rate of 100 mV/s was applied to a three electrode cell constructed using a Ag/AgCl reference electrode and Pt wire counter electrode in 0.1 M Bu<sub>4</sub>NPF<sub>6</sub>, N-dimethylformamide solution. Ferrocene was then used to calibrate the system. In the frequency range 0.1 to 100 kHz an Electrochemical Workstation (CH-604D) was applied a dc biasing equivalent to the open circuit voltage. The resulting electrochemical impedance spectra (EIS) were recorded under dark conditions.

### 3 Results and Discussion

The metal free dye TA-St-CA was synthesized using a previously reported method<sup>41</sup>. The dye TA-St-CA contains triphenylamine as donor and cyanoacrylic acid as acceptor moiety and a  $\pi$ -conjugated oligophenylene unit used as co-sensitizer along with the well known Ru based dye, i.e., N719. The chemical structure of TA-St-CA and N719 are shown in Fig. 1. The dye TA-St-CA showed absorption maxima around 412 nm with molar extinction coefficient<sup>42</sup>  $2.8 \times 10^4 \text{ M}^{-1} \text{ cm}^{-1}$ . The Ruthenium complex dye, N719, was adopted as the primary sensitizer because it is commonly used and has a wide

Fig. 2 – (a) Absorption spectra TA-St-CA and N719 of in solution, (b) normalized absorption spectra of TA-St-CA, N719 and N719/TA-St-CA adsorbed onto TiO<sub>2</sub> film

absorption range. N719 dye showed visible region absorption peaks located at wavelengths of 540 nm (molar extinction coefficient  $2.0 \times 10^4 \text{ M}^{-1} \text{ cm}^{-1}$ ) and 380 nm (molar extinction coefficient  $2.5 \times 10^4 \text{ M}^{-1} \text{ cm}^{-1}$ ) and attributed to charge transfer (MLCT) associated with the metal-ligand transition and the  $\pi$ - $\pi^*$  transition contribution, respectively.

The absorption spectrum of N719, TA-St-CA and N719/TA-St-CA adsorbed onto TiO<sub>2</sub> film are shown in Fig. 2. It can be seen from this figure that the

TA-St-CA dye adsorbed onto TiO<sub>2</sub> film poses an absorption peak around 430 nm, where N719 possesses the dip in the absorption spectrum. The N719/TA-St-CA dye system shows a broad absorption spectrum covering a wide range in the visible region extending up to 780 nm with superior light harvesting efficiency compared to the individual dyes.

Figure 3 shows the current-voltage (*J-V*) characteristics of DSSC's manufactured using the individual dyes, N719 and TA-St-CA, and the cosensitized systems prepared using N719/TA-St-CA and TA-St-CA/N719 (in the orders shown), respectively. The corresponding photo voltaic parameters are given in Table 1. The DSSC manufactured using the TA-St-CA sensitizer yielded a  $J_{sc}$ ,  $V_{oc}$ ,  $FF$  and  $PCE$  of 10.23 mA/cm<sup>2</sup>, 0.64 V, 0.68 and 4.45%, respectively. In comparison the cell sensitized with N719 yielded values of  $J_{sc}$ ,  $V_{oc}$ ,  $FF$  and  $PCE$  of 13.14 mA/cm<sup>2</sup>, 0.62 V, 0.71, and 5.78%, respectively. However, the DSSCs cosensitized with (N719/TA-St-CA) showed a greater performance increase ( $J_{sc}$ =16.22 mA/cm<sup>2</sup>,  $V_{oc}$ = 0.68 V,  $FF$  = 0.75 and  $PCE$  = 8.27%) when compared to the cells sensitized using the individual dyes N719 and TA-St-CA. This improvement was apparent in both  $J_{sc}$  and  $V_{oc}$ . A higher  $J_{sc}$  was recorded for the cosensitized DSSCs

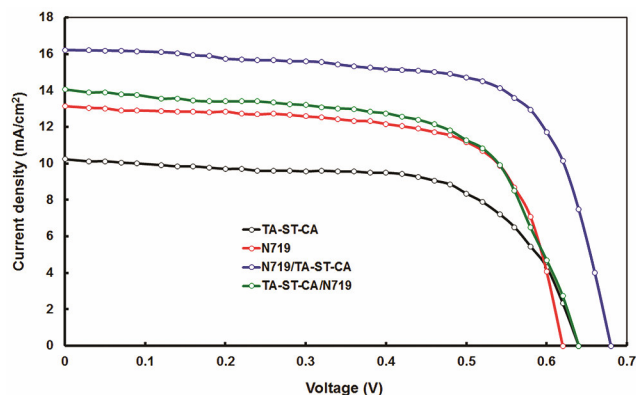


Fig. 3 – Current-voltage (*J-V*) characteristics of cosensitized (N719/TA-St-CA and TA-St-CA/N719) DSSCs and those sensitized with TA-St-CA and N719, under illumination (100 mW/cm<sup>2</sup>)

Table 1 – Photovoltaic parameters of the DSSCs based on different dye systems

Dye	$J_{sc}$ (mA/cm <sup>2</sup> )	$V_{oc}$ (V)	$FF$	$PCE$
TA-St-CA	10.23	0.64	0.68	4.45
N719	13.14	0.62	0.71	5.78
N719/TA-St-CA	16.22	0.68	0.75	8.27
TA-St-CA/N719	14.06	0.64	0.68	6.12

(N719/TA-St-CA) when a comparison was made to the individual dyes. Charge collection, light harvesting efficiency and charge separation (electron injection, regeneration and recombination) were all found to influence the  $J_{sc}$ . Other research groups have reported that the breakup of dye aggregates is associated with the cosensitization of dyes with co-adsorbents. This was found to yield higher values<sup>17</sup> of both  $J_{sc}$  and  $V_{oc}$ .

Figure 4 shows the DSSC's IPCE spectra. It can be seen from the IPCE spectrum of the DSSC sensitized with N719 dye, that there is a decrease in the wavelength region 400-430 nm, which is attributed to competition of absorption between the  $I_3^-$  and N719 dye, since the  $I_3^-$  showed a higher molar extinction coefficient compared to the N719 in this wavelength region. Compared to  $I_3^-$ , the TA-St-CA dye showed a much higher molar extinction coefficient (greater ability for light harvesting) throughout this region, the dip is recovered in the IPCE spectra of DSSC based on N719/TA-St-CA cosensitized dye. Therefore we expect that the reduction of the light absorption by  $I_3^-$  to be suppressed by the co-adsorbent TA-St-CA.

Recovery of the dip in the IPCE spectra of DSSC sensitized with N719 near 410 nm is due to the competitive absorption of light by  $I_3^-$ . It is also required that the electrons are injected easily from the co-sensitizer LUMO level into the conduction band of the TiO<sub>2</sub>. Cyclic voltammetry and density functional theory (DFT) calculations, reported earlier<sup>41</sup>, were used to estimate the HOMO, (highest occupied

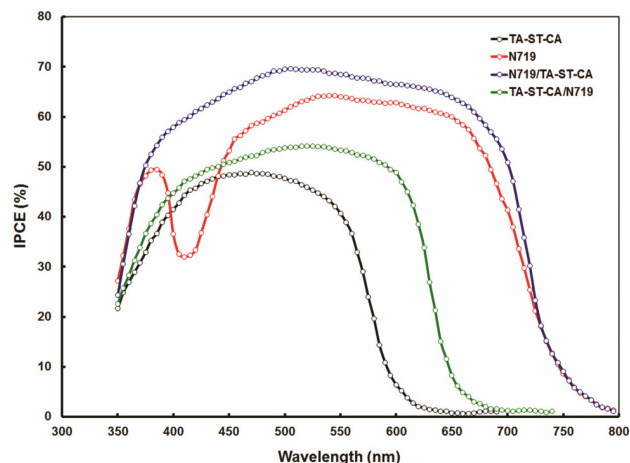


Fig. 4 – IPCE spectra of DSSCs sensitized with TA-St-CA, N719, N719/TA-St-CA and TA-St-CA/N719

molecular orbital) and LUMO (lowest unoccupied molecular orbital) levels of both the dyes. The higher excited state oxidation potentials, i.e., LUMO energy level of TA-St-CA (-3.53 eV), compared to the conduction band edge (-4.2 eV) of nano-crystalline TiO<sub>2</sub> facilitate the electrons injection from the TA-St-CA co-sensitizer into the TiO<sub>2</sub> conduction band. Moreover, the lower HOMO level of TA-St-CA compared to the redox potential of  $I^-/I_3^-$  effectively regenerate the oxidized TA-St-CA.

The DSSC sensitized with N719 dye alone had a broadband IPCE spectra extending across the whole visible region and into the near infrared region up to 750 nm and showed the highest average IPCE value of 53% in the wavelength region 470–670 nm. As discussed earlier, the IPCE value decrease of up to 32% at the wavelength 410 nm was attributed to the competitive light absorption of  $I_3^-$  and N719 dye. When the DSSC is co-sensitized with TA-St-CA, i.e., N719/TA-St-CA system, the dip in the IPCE spectrum is recovered. This observation is in agreement with the IPCE spectra of DSSCs based on TA-St-CA alone. This is also consistent with the absorption spectra of TA-St-CA dye adsorbed on the TiO<sub>2</sub> film (Fig. 4(b)). The values of the IPCE are also higher for the DSSC sensitized with N719/TA-St-CA compared to N719, in the wavelength range 370–730 nm. The increase in the light harvesting efficiency, electron injection from the both the dyes, i.e., N719 and TA-St-CA into the conduction band of TiO<sub>2</sub> contribute to the higher values of  $J_{sc}$  and overall PCE of the DSSC sensitized with the N719/TA-St-CA system.

We have also investigated the DSSCs sensitized with TA-St-CA/N719, i.e., sensitization of TiO<sub>2</sub> electrode first dipping in the TA-St-CA followed by the N719 dye. The current-voltage ( $J$ - $V$ ) characteristics and IPCE spectra of this device is also shown in Figs 3 and 4 and the photovoltaic parameters are also shown in Table 2. It can be seen that the cosensitized (TA-St-CA/N719) DSSC showed slightly improved performance ( $J_{sc} = 14.06$  mA/cm<sup>2</sup>,  $V_{oc} = 0.64$ ,  $FF = 0.68$  and  $PCE = 6.12\%$ ) compared to the DSSC sensitized with N719.

To get more information about the origin of the enhancement in the  $J_{sc}$  of the cosensitized dye based DSSCs, UV-visible absorption spectroscopy has been carried out to study light harvesting properties of cosensitization. Figure 2(a) shows the absorption

Table 2 – EIS parameters and charge collection efficiency of DSSCs using different dyes

Dye system	$R_f$ (Ohm/cm <sup>2</sup> )	$R_{ct}$ (Ohm/cm <sup>2</sup> )	$\tau_n$ (ms)	$\eta_{cc}$
TA-St-CA	14.3	38	26	0.73
N719	13.6	53	34	0.79
N719/TA-St-CA	9.8	85	57	0.90

spectra of TA-St-CA and N719 in solution and Fig. 2(b) shows the absorption spectra of the TA-St-CA, N719 and N719/TA-St-CA cosensitized system, adsorbed onto 4  $\mu$ m nanocrystalline TiO<sub>2</sub> films made from DL18-NRT TiO<sub>2</sub> paste. Both the spectra clearly demonstrate that TA-St-CA dye possesses the higher absorption intensity in 400–470 nm where the N719 shows lower absorption. Therefore, upon cosensitization, i.e., N719/TA-St-CA, the absorption spectra of the cosensitized film demonstrates a panchromatic feature to provide an increased light harvesting efficiency. Apart from the absorption profile, the amount of dye loading is an important factor for enhanced PCE of the DSSCs. To estimate the amount of dye loading on the TiO<sub>2</sub> film, the amount of dye adsorbed on to the 12  $\mu$ m thick TiO<sub>2</sub> film was measured. First the cosensitized TiO<sub>2</sub> electrode was dipped into 0.05 M NaOH solution, desorption of TA-St-CA occurs predominantly compared to that of N719. The amounts of TA-St-CA desorbed were estimated by measuring the absorption spectra of the NaOH solution and monitoring the absorption peak at 420 nm, effectively measuring the absorption of the desorbed TA-St-CA. The residual N719 dye on the photoanode was then determined by dipping in acetonitrile/tert-butanol (1:1 v/v) and then measuring the absorption spectra of this solution. The amount of N719 was measured by monitoring the absorption peak at 530 nm. The amounts of N719 dye and TA-St-CA on the N719/TA-St-CA cosensitized TiO<sub>2</sub> electrode were  $1.45 \times 10^{-7}$  mole/cm<sup>2</sup> and  $0.96 \times 10^{-7}$  mole/cm<sup>2</sup>, respectively. It is noted that the concentration of TA-St-CA on the cosensitized N719/TA-St-CA TiO<sub>2</sub> electrode is less than the TiO<sub>2</sub> sensitized with TA-St-CA ( $1.67 \times 10^{-7}$  mole/cm<sup>2</sup>) alone, indicating that there is a lower number of binding sites left on the TiO<sub>2</sub> surface after N719 adsorption<sup>43,44</sup>. But the total number of the N719 dye for N719/TA-St-CA cosensitized photoanode is almost same as for the individual N719 sensitized photoanode. In spite of that the total number of dye molecules (both N719 and TA-St-CA) significantly increased to  $2.4 \times 10^{-7}$  mole/cm<sup>2</sup>. These results

demonstrate that the total dye coverage had been improved by inserting the small molecular sized TA-St-CA molecules into the gaps left after the sensitization of N719. Moreover, N719 dye adsorbed with the TiO<sub>2</sub> surface via its carboxylic anchoring groups, whereas TA-St-CA dye is adsorbed through not only carboxylic groups but also via nitrogen in the cyano group<sup>45</sup>. Therefore, the anchoring sites on TiO<sub>2</sub> nanoparticles are different for two dyes, thus enhancing their absorption-dispersion on the TiO<sub>2</sub> surface<sup>46</sup>.

It can be seen from the J-V characteristics of the DSSC cosensitized with TA-St-CA/N719 under illumination, Table 1, that the value of  $J_{sc}$  and PCE are 14.06 mA/cm<sup>2</sup> and 6.12 %. These values are significantly less than that for the N719/TA-St-CA sensitized DSSC and higher than that sensitized with either individual N719 or TA-St-CA dye sensitized DSSC. We have also measured the dye loading for photoanodes sensitized with TA-St-CA employing same methods as described above and found that the amount of N719 dye adsorbed onto the TiO<sub>2</sub> surface ( $0.67 \times 10^{-7}$  mol/cm<sup>2</sup>) for the TA-St-CA/N719 system is much smaller than that for N719/TA-St-CA and the amount of TA-St-CA is about  $1.7 \times 10^{-7}$  mol/cm<sup>2</sup>. Since in the TA-St-CA/N719, first the TA-St-CA dye was adsorbed on the TiO<sub>2</sub> surface and then the N719 dye, the larger molecular size of N719 does not allow full adsorption onto the TiO<sub>2</sub> surface on the gap left after TA-St-CA sensitization. The lower amount the N719 dye adsorbed may be attributed to the lower value of  $J_{sc}$  and overall PCE. The shape of the IPCE spectra of the DSSC based on TA-St-CA/N719 is also consistent with the observed value of  $J_{sc}$ .

Apart from the increase in  $J_{sc}$ , the  $V_{oc}$  also increased for the cosensitized DSSC. To clarify the effect of cosensitizer on  $V_{oc}$ , electrochemical impedance spectroscopy (EIS) was performed under dark conditions. The  $V_{oc}$  of a DSSCs can be defined as the difference in voltage between the electrolyte redox potential ( $E_{redox/q}$ ) and quasi Fermi potential of electrons ( $E_{F,n}$ ) in the TiO<sub>2</sub>. Improvements in  $V_{oc}$  can usually be attributed to suppression of charge recombination and a negative shift in the conduction band edge.

The following expression<sup>47</sup> is commonly used to define  $V_{oc}$ :

$$V_{oc} = E_{CB} / q + \frac{kT}{q} \ln \left( \frac{n}{N_{CB}} \right) - \frac{E_{redox}}{q}$$

where  $E_{CB}$ ,  $q$ ,  $n$  and  $N_{CB}$  denote the TiO<sub>2</sub> conduction band edge, electronic charge, number of electrons in the TiO<sub>2</sub> conduction band and the density of states in the conduction band respectively. Within this study it is assumed that the ratio of  $E_{redox}/q$  is constant because the same electrolyte was used in all the cells.

The value of  $V_{oc}$  is determined by the conduction band edge and the electron concentration in the conduction band of TiO<sub>2</sub> both of these parameters are sensitive to the type of dye which is used as a sensitizer in the cell. Surface charges introduced by species such as dye molecules, additives, co-absorbents and ions all influence the position of the conduction band. The conduction band edge will vary when there is a change in surface charge, which by definition also influences  $V_{oc}$ . The balance between the electron recombination and injection will define the number of electrons. Improvements in  $V_{oc}$  could also be related to an increase in  $J_{sc}$ , which is expressed by the following equation<sup>48</sup>:

$$V_{oc} = \left( \frac{\gamma kT}{q} \right) \ln \left( \frac{J_{sc}}{J_{dark}} \right)$$

where  $\gamma$ ,  $k$ ,  $T$ ,  $J_{dark}$  are the ideality factor, Boltzmann's constant, temperature, and  $J_{dark}$  is dark current, respectively. It can be seen from above expression that the  $V_{oc}$  depends upon the  $\ln(J_{sc}/J_{dark})$ , indicating that the increase in  $V_{oc}$  can be attributed to the increased electron density in the conduction band of TiO<sub>2</sub> which is caused by the photoinduced electron injection from the dyes LUMO levels. In the case of cosensitization, both the N719 and TA-St-CA dye are injecting electrons into the TiO<sub>2</sub> conduction band leading to enhancement in the electron density in the TiO<sub>2</sub>, resulting in improvement in  $J_{sc}$ . The value of  $J_{sc}$  is significantly improved for cosensitized N719/TA-St-CA, but the increase in  $V_{oc}$  is of the same order. This is attributed to the recombination between the injected electrons from the dyes into the conduction band of the TiO<sub>2</sub> and  $I_3^-$  in the electrolyte, which is not completely suppressed although it was suppressed for the cosensitized system.

As discussed above, the cosensitization of N719/TA-St-CA, resulted in enhancement of the PCE in DSSCs which is believed to be due to the enhancement in  $J_{sc}$ ,  $FF$  and  $V_{oc}$ . This enhancement was expected to result from improved light harvesting efficiency due to the adsorption of two dyes onto the



TiO<sub>2</sub> surface and reduced dark current due to the dense packing of the two dyes on the surface. In addition reduced dye aggregation on the TiO<sub>2</sub> electrode was expected because of the different anchoring sites for N719 and TA-St-CA. To investigate the second effect further, we have recorded the *J-V* characteristics of the DSSCs in the dark as shown in Fig. 5. The dark current is suppressed significantly in the N719/TA-St-CA cosensitized system. Since dark current in DSSCs is a measure of recombination between the injected electrons with  $I_3^-$  ions in electrolyte the decrease is attributed to the low recombination rate between the injected electrons in conduction band of TiO<sub>2</sub> with  $I_3^-$  and to the higher coverage of the TiO<sub>2</sub> surface due to the increased overall dye loading. This decrease in dark current contributes to an increase in  $V_{oc}$  for DSSCs based on N719/TA-St-CA.

The photoanode electron transfer and recombination processes are elucidated from the EIS data in this investigation<sup>49-51</sup>. Nyquist and Bode phase plots for the DSSCs based on different sensitizers measured by EIS at a forward bias of 0.65 V, in the dark, are given in Fig. 6. Three semicircles are visible on the Nyquist plots produced from the EIS data. The far left semicircle corresponds to the impedances of charge transfer at the Pt counter electrode (high frequency range), the central semicircle to the charge transfer and recombination competition at the TiO<sub>2</sub>/dye/electrolyte interface (middle frequency range), and the right hand side semicircle to the electrolyte diffusion (low frequency range). The kinetics of the charge transfer process at the electrolyte/dye/TiO<sub>2</sub> interface is expressed by the large middle frequency circle of the Nyquist plot. The semicircle corresponding to the DSSC sensitized with N719/TA-St-CA is larger when compared to that of the individual N719 or TA-St-CA dyes. This centrally located semicircle has been identified to help understand the interfacial charge transfer process and recombination resistance ( $R_{ct}$ ). Figure 6(b) is a Bode phase plot from which it is possible to estimate the peak frequency and therefore electron lifetime using the expression  $\tau_n = 1/2\pi f_{max}$ , in addition to information on the recombination resistance ( $R_{ct}$ ). The expression

$\eta_{cc} = (1 + R_t / R_{ct})^{-1}$  was used to estimate the charge collection efficiency where the electron transport resistance is denoted by  $R_t$ . Within the central semicircle consideration of the high frequency

region reveals a linear feature which is attributed to the electron transport resistance ( $R_t$ ). This is in agreement with work by Bisquert on DSSC's with photoanodes, which suggests that a transmission line behavior is shown in the electron transport<sup>52,53</sup>. Table 2 summarizes the parameters  $R_{ct}$ ,  $R_t$ ,  $\tau_n$  and  $\eta_{cc}$  which were calculated from an equivalent circuit diagram based on the transmission line model. The DSSC's

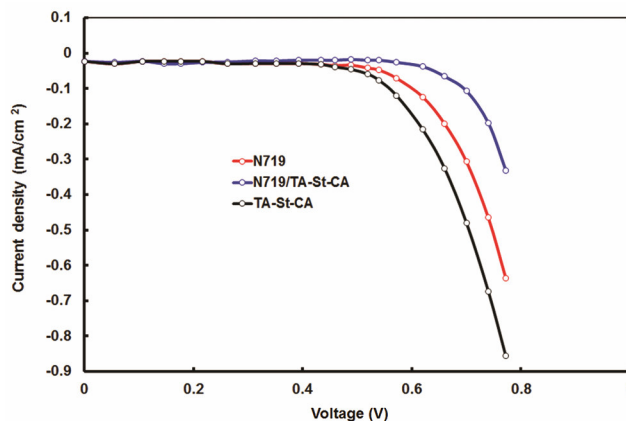


Fig. 5 – Current-voltage characteristics of DSSCs based on N719, TA-St-CA and N719/TA-St-CA, under dark conditions

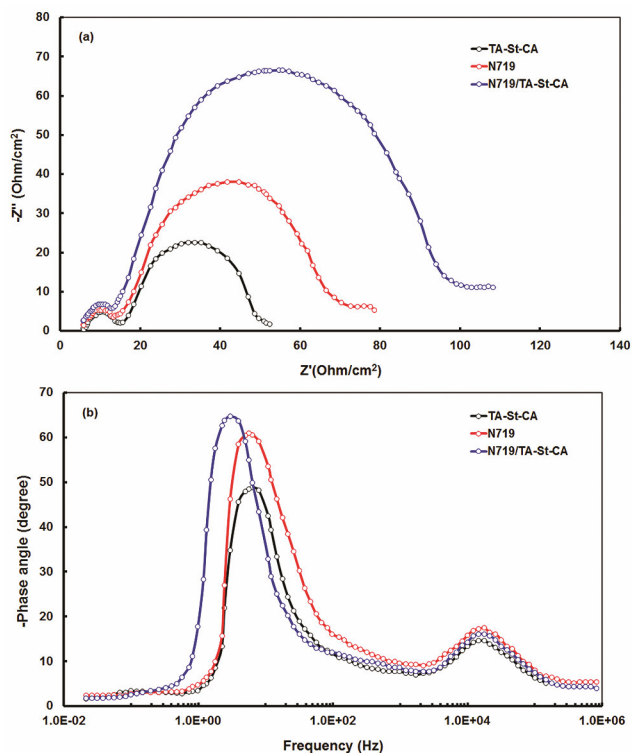


Fig. 6 – (a) Nyquist and (b) Bode phase plots from the EIS spectra for the DSSCs sensitized with TA-St-CA, N719 and N719/TA-St-CA in dark conditions



based on N719/TA-St-CA dyes exhibited a higher resistance to recombination compared to the cells sensitized with dyes N719 and TA-St-CA individually. The work of Bhaers suggests that changes in the efficiency of electron injection may be attributed to changes in the electronic states of the dye sensitized TiO<sub>2</sub> and the adsorption state of the dye induced by cosensitization<sup>46</sup>. It therefore follows that improvements in the  $J_{sc}$  for DSSC's cosensitized with N719/TA-St-CA compared to the individual dyes N719 or TA-St-CA may be attributed to the breakup of aggregated dyes from competition between co-adsorbed N719 and TA-St-CA.

#### 4 Conclusions

We have used a stepwise cosensitization process using N719 and metal free dye, i.e., TA-St-CA to improve the PCE of the DSSCs. Significant improvements in the PCE have been observed for N719/TA-St-CA (8.27%) based DSSCs compared to those sensitized with individual either N719 (5.78%) or TA-St-CA (4.45%). This was attributed to the enhancement in the light harvesting efficiency, overall dye loading and reduction in dye aggregation. In addition, the combination of the two dyes with different anchoring units, results in larger coverage of TiO<sub>2</sub> surfaces, thereby enhancing the  $J_{sc}$  and reducing the back electron recombination with  $I_3^-$  in the electrolyte, which in turn increases the overall power conversion efficiency.

#### Acknowledgement

Manjeet Singh is grateful to Maulana Azad National Institute of Technology (MANIT), Bhopal, India for Institute Fellowship for supporting his doctoral degree. Authors are thankful to UK India Education and Research Initiative (UKIERI-II) coordinated by the British Council, New Delhi, India for financial support through a Thematic Partnership. Authors are also thankful to Petra J Cameron, Department of Chemistry, University of Bath, UK, for providing some fabrication and characterization facilities.

#### References

- 1 Regan B O & Gratzel M, *Nature*, 353 (1991) 737.
- 2 Gratzel M, *Nature*, 414 (2001) 338.
- 3 Wu Y & Zhu W, *Chem Soc Rev*, 42 (2013) 2039.
- 4 A Yella, Lee H-W, Tsao H N, Yi C, Chandiran A K, Nazeeruddin M K, Diao E W-G, Yeh C-Y, Zakeeruddin S M & Gratzel M, *Science*, 334 (2011) 629.
- 5 Zhang S, Yang X, Numata Y & Han L, *Energy Environ Sci*, 6 (2013) 1443.
- 6 Hagfeldt A, Boschloo G, Sun L, Kloo L & Pettersson H, *Chem Rev*, 110 (2010) 6595.
- 7 Jiao Y, Zhang F, Gratzel M & Meng S, *Adv Funct Mater*, 23 (2013) 424.
- 8 Kim B H & Freeman H S, *Photochem Photobiol Sci*, 12 (2013) 421.
- 9 Kim B H & Freeman H S, *J Mater Chem*, 22 (2012) 20403.
- 10 Gao F, Wang Y, Shi D, Zhang J, Wang M, Jing X, Humphry-Baker R, Wang P, Zakeeruddin S M & Gratzel M, *J Am Chem Soc*, 130 (2008) 10720.
- 11 Cao Y, Bai Y, Yu Q, Cheng Y, Liu S, Shi D, Gao F & Wang P, *J Phys Chem C*, 113 (2009) 6290.
- 12 Reynal A, Forneli A & Palomares E, *Energy Environ Sci*, 3 (2010) 805.
- 13 Campbell W M, Jolley K W, Wagner P, Wagner K, Walsh P J, Gordon K C, Schmidt-Mende L, Nazeeruddin M K, Wang Q & Officer D L, *J Phys Chem C*, 111 (2007) 11760.
- 14 Wang C L, Lan C M, Hong S H, Wang Y F, Pan T Y, Chang C W, Kuo H H, Kuo M Y, Diao E W G & Lin C Y, *Energy Environ Sci*, 5 (2012) 6933.
- 15 Li Lu-Lin & Diao Eric Wei-Guang, *Chem Soc Rev*, 42 (2013) 291.
- 16 Mishra A, Fischer M K R & Bauerle P, *Angew Chem, Int Ed*, 48 (2009) 2474.
- 17 Kim B-G, Zhen C-G, Jeong E J, Kieffer J & Kim J S, *Adv Funct Mater*, 22 (2012) 1606.
- 18 Kim Bong-Gi, Chung K & Kim J, *Chem Eur J*, 19 (2013) 5220.
- 19 Nazeeruddin M K, Péchy P, Grätzel M, *Chem Commun*, 85 (1997) 1705.
- 20 Koumura N, Wang Z-S, Mori S, Miyashita M, Suzuki E & Hara K, *J Am Chem Soc*, 128 (2006) 14256.
- 21 Peter L M, *J Phys Chem Lett*, 2 (2011) 1861, Yum J-H, Baranoff E, Wenger S, Nazeeruddin M K & Gratzel M, *Energy Environ Sci*, 4 (2011) 842.
- 22 Abbotto A, Sauvage F, Barolo C, Angelis F De, Fantacci S, Gratzel M, Manfredi N, Marini C & Nazeeruddin M K, *Dalton Trans*, 40 (2011) 234.
- 23 Paek S, Choi H, Kim C, Cho N, So S, Song K, Nazeeruddin M K & Ko J, *Chem Commun*, 47 (2011) 2874.
- 24 Robertson N, *Angew Chem*, 47 (2008) 012.
- 25 Choi H, Kim S, Kang S O, Ko J, Kang M-S, Clifford J N, Forneli A, Palomares E, Nazeeruddin M K & Gratzel M, *Angew Chem*, 47 (2008) 8259.
- 26 Ogura R Y, Nakane S, Morooka M, Orihashi M, Suzuki Y & Noda K, *Appl Phys Lett*, 94 (2009) 073308
- 27 Bessho T, Zakeeruddin S M, Yeh C-Y, Diao E W-G & Gratzel M, *Angew Chem*, 49 (2010) 6646.
- 28 Lan C-M, Wu H-P, Pan T-Y, Chang C-W, Chao W-S, Chen C-T, Wang C-L, Lin C-Y & Diao E W-G, *Energy Environ Sci*, 5 (2012) 6460.
- 29 Zhang S, Islam A, Yang X, Qin C, Zhang K, Numata Y, Chen H & Han Liyuan, *J Mater Chem A*, 1 (2013) 4812.
- 30 Han L, Islam A, Chen H, Malapaka C, Chiranjeevi B, Zhang S, Yang X & M Yanagida, *Energy Environ Sci*, 5 (2012) 6057.
- 31 Wang M, Chamberland N, Breau L, Moser J, Humphry-Baker R, Marsa B, Zakeeruddin S M & Gratzel M, *Nat Chem*, 2 (2010) 385

- 32 Lee C L, Lee W H & Yang C H, *J Mater Sci*, 48 (2013) 3448.
- 33 Miao Q, Wu L, Cui J, Huang M & Ma T, *Adv Mater*, 23 (2011) 2764.
- 34 Zhao W, Hou Y J, Wang X S, Zhang B W, Cao Y, Yang R, Wang W B & Xiao X R, *Sol Energy Mater Sol Cells*, 58 (1999) 173.
- 35 Zhang D S, Wang W B, Liu Y, Xiao X R, Zhao W, Zhang B W & Cao Y, *J Photochem Photobiol*, 135 (2000) 235.
- 36 Sayama K, Tsukagoshi S, Mori T, Hara K, Ohga Y, Shinpou A, Abe Y, Suga S & Arakawa H, *Sol Energy Mater Sol Cells*, 80 (2003) 47.
- 37 Xue Z, Wang L & Liu B, *Nanoscale*, 5 (2013) 2269.
- 38 Kuang D, Walter P, Nuesch F, Kim S, Ko J, Comte P, Zakeeruddin S M, Nazeeruddin M K & Gratzel M, *Langmuir*, 23 (2007) 10906.
- 39 Fan S-Q, Kim C, Fang B, Liao K-X, Yang G-J, Li C-J, Kim J-J & Ko J, *J Phys Chem C*, 115 (2011) 7747.
- 40 Lee Kun-Mu, Hsu Ying-Chan, Ikegami M, Miyasaka T, Thomas K R J, Lin J T & Ho Kuo-Chuan, *J Power Source*, 196 (2011) 2416.
- 41 Akhtaruzzaman M, Islam A, Yang F, Asao N, Kwon E, Singh S P, Han L & Yamamoto Y, *Chem Commun*, 47 (2011) 12400.
- 42 Sharma G D, Singh S P, Nagarjuna P, Mikroyannidis J A, Ball R J & Kurchania R, *J Renewable Sustainable Energ*, 5 (2013) 043107.
- 43 Song B J, Song H M, Choi I T, Kim S K, Seo K D, Kang M S, Lee M J, Cho D W Ju, M J & Kim H K, *Chem-Eur J*, 17 (2011) 11115.
- 44 Kang M S, Kang S H, Kim S K, Choi I T, Ryu J H, Ju M J, Cho D W, Lee J Y & Kim H K, *Chem Commun*, 48 (2012) 9349.
- 45 Ogura R Y, Nakane S, Morooka M, Orihashi M, Suzuki Y & Noda K, *Appl Phys Lett*, 94 (2009) 073308.
- 46 Bahers T Le, Pauporte T, Scalmani G, Adamo C & Ciofini I, *Phys Chem Chem Phys*, 11 (2009) 11276.
- 47 Green M A, *Solar Cells: Operating Principles, Technology, and System Applications*, Prentice-Hall, Englewood Cliffs, NJ, 1982
- 48 Yanagida M, Yamaguchi T, Kurashige M, Hara K, Katoh R, Sugahara H, Arakawa H, *Inorg Chem*, 42 (2003) 7921.
- 49 Kern R, Sastrawan R, Ferber J, Stangl R & Luther J, *Electrochim Acta*, 47 (2002) 4213, Bisquert J, *J Phys Chem B*, 106 (2002) 325.
- 50 Fabregat-Santiago F, Bisquert J, Cevey L, Chen P, Wang M, Zakeeruddin S M & Gratzel M, *J Am Chem Soc*, 131 (2009) 558.
- 51 Wang Q, Zhang Z, Zakeeruddin S M & Gratzel M, *J Phys Chem C*, 112 (2008) 7084.
- 52 Bisquert J, *J Phys Chem B*, 106 (2002) 325.
- 53 Bisquert J, Fabregat-Santiago F, Mora-Sero I, Garcia-Belmonte G & Gimenez S J, *J Phys Chem C*, 113 (2009) 1727.